

KEYWORDS:

Saltstone
PORFLOW
Vadose Flow
Vadose Transport

RETENTION

Permanent

SDU 6 Modeling Study to Support Design Development

F. G. Smith, III

MAY 2, 2012

Savannah River National Laboratory
Savannah River Nuclear Solutions
Savannah River Site
Aiken, SC 29808

**Prepared for the U.S. Department of Energy Under
Contract Number DE-AC09-08SR22470**



DISCLAIMER

This work was prepared under an agreement with and funded by the U.S. Government. Neither the U. S. Government or its employees, nor any of its contractors, subcontractors or their employees, makes any express or implied:

- 1. warranty or assumes any legal liability for the accuracy, completeness, or for the use or results of such use of any information, product, or process disclosed; or**
- 2. representation that such use or results of such use would not infringe privately owned rights; or**
- 3. endorsement or recommendation of any specifically identified commercial product, process, or service.**

Any views and opinions of authors expressed in this work do not necessarily state or reflect those of the United States Government, or its contractors, or subcontractors.

Printed in the United States of America

Prepared For

U.S. Department of Energy

KEYWORDS:

Saltstone
PORFLOW
Vadose Flow
Vadose Transport

RETENTION

Permanent

SDU 6 Modeling Study to Support Design Development

F. G. Smith, III

MAY 2, 2012

Savannah River National Laboratory
Savannah River Nuclear Solutions
Savannah River Site
Aiken, SC 29808

**Prepared for the U.S. Department of Energy Under
Contract Number DE-AC09-08SR22470**



TABLE OF CONTENTS

1.0 EXECUTIVE SUMMARY 1

 1.1 MODELING APPROACH..... 1

 1.2 QUALITY ASSURANCE..... 1

 1.3 SUMMARY OF RESULTS..... 1

2.0 INTRODUCTION..... 2

 2.1 BACKGROUND..... 2

3.0 MODELING..... 3

 3.1 APPROACH..... 3

 3.2 MODEL DESCRIPTION..... 5

 3.3 MESH2D..... 6

 3.4 INFILTRATION 7

4.0 MODEL RESULTS 8

 4.1 FLOW RESULTS 8

 4.2 TRANSPORT RESULTS 8

5.0 CONCLUSIONS 17

 5.1 MODEL IMPROVEMENTS 17

6.0 REFERENCES..... 18

APPENDIX A ESTIMATION OF INITIAL WALL DEGRADATION..... 19

APPENDIX B EQUIVALENT GRAVEL FLOW PATH FOR ROOF AND FLOOR JOINTS 21

APPENDIX C MODEL RUNS WITHOUT ROOF AND FLOOR JOINTS..... 22

APPENDIX D DESIGN CHECK DOCUMENTATION 25

LIST OF TABLES

Table 1. Case Studies for SDU 6 Modeling.....	2
Table 2. Predicted times to concrete failure.....	4
Table 3. Materials used in SDU 6 model.....	6
Table 4. Peak flux to water table and year of occurrence for SDU 6 Base Case and Vault 2 Case A.....	15
Table 5. Peak flux to water table and year of occurrence for SDU 6 Sensitivity Cases.....	16

LIST OF FIGURES

Figure 1. Computational model of SDU6 showing material zones.	5
Figure 2. Infiltration and hydraulic conductivity.....	7
Figure 3. Flow streamlines and pressure contours at 500 years for Base Case calculations. .	8
Figure 4. Flux to water table of I-129 from SDU 6.	10
Figure 5. Flux to water table of Np-237 from SDU 6.....	10
Figure 6. Flux to water table of Pa-231 from SDU 6.....	11
Figure 7. Flux to water table of Pa-231 as daughter of U-235 from SDU6.....	11
Figure 8. Flux to water table of Tc-99 from SDU 6.	12
Figure 9. Flux to water table of Ra-226 as parent from SDU 6.....	12
Figure 10. Flux to water table of Ra-226 as daughter of U-234 from SDU 6.	13
Figure 11. Flux to water table of Ra-226 as daughter of Pu-238 from SDU 6.....	13
Figure 12. Flux to water table of Ra-226 as daughter of Th-230 from SDU 6.....	14
Figure C1. Flux to water table of Np-237 from SDU 6 with and without roof and floor joints compared to flux from Vault 2.....	22
Figure C2. Flux to water table of Pa-231 from SDU 6 with and without roof and floor joints compared to flux from Vault 2.....	23
Figure C3. Flux to water table of Tc-99 from SDU 6 with and without roof and floor joints compared to flux from Vault 2.....	23
Figure C4. Flux to water table of Ra-226 from SDU 6 with and without roof and floor joints compared to flux from Vault 2.....	24

1.0 Executive Summary

1.1 Modeling Approach

SRR requested that SRNL assess alternative design options for Saltstone Disposal Unit (SDU) 6 by performing PORFLOW modeling to calculate the release of key radionuclides from SDU 6. Because a quick response was needed that would be adequate for evaluation of design alternatives, the PORFLOW analysis was limited to calculating radionuclide fluxes to the water table through the vadose zone for the key radionuclides identified by the 2009 Saltstone Performance Assessment (PA) over a 15,000 year time period. Results are compared to those obtained from the previous Vault 2 Case A design. However, because the analysis did not include aquifer transport and a calculation of maximum concentration and dose at a hypothetical well 100 m from the facility boundary, the comparison of SDU 6 to Vault 2 is only semi-quantitative.

1.2 Quality Assurance

This work was performed in response to Technical Task Request (TTR) HLW-SSF-TTR-2012-0017. In compliance with SRNL QA procedures, a TTQAP “Task Technical and Quality Assurance Plan for SDU 6 Modeling Study to Support Design Development,” SRNL-RP-2012-00061, Rev. 0, February 9, 2012 was issued. The modeling calculations used the commercial Computational Fluid Dynamics (CFD) code PORFLOW Version 6.30.2. PORFLOW has been used in previous PA and Special Analysis calculations performed at SRNL. The calculations reported here relied in large part on the previous saltstone calculations made in the 2009 PA for material properties, estimation of concrete degradation, and the general modeling approach. In addition, an independent design check of the PORFLOW models and supporting calculations was performed as documented in Appendix D.

1.3 Summary of Results

In general, when compared to Vault 2 Case A, the Base Case SDU 6 design produced higher peak fluxes to the water table during the 10,000 year period of analysis but lower peak fluxes within a 15,000 to 20,000 time frame. This was primarily caused by the modeling of floor joints in the SDU 6 design and the relatively thin five-inch floor thickness in the SDU 6 design both of which created pathways for radionuclide releases at early times. The five-inch floor was fully degraded at 8,000 years which caused a spike in fluxes at that point. In contrast, the Vault 2 design had a similar spike in flux at 15,000 years when the wall hydraulic conductivity significantly increased. The analysis did not show a significant difference in performance when the vault roof thickness was increased or when the total length of joints in the roof and floor were halved from 2,000 linear feet to 1,000 linear feet. Increasing the floor thickness to 10 inches eliminated the flux spike at 8,000 years. Reducing the distance from the vault floor to the water table by 20 ft led to an increase in flux by approximately a factor of two for Ra-226 and less for other nuclides. Additional more detailed modeling is already in the planning stage.

2.0 Introduction

2.1 Background

In response to Technical Task Request (TTR) HLW-SSF-TTR-2012-0017 (1), SRNL performed modeling studies to evaluate alternative design features for the 32 million gallon Saltstone Disposal Unit (SDU) referred to as SDU 6. This initial modeling study was intended to assess the performance of major components of the structure that are most significant to the PA. Information provided by the modeling will support the development of a SDU 6 Preliminary Design Model and Recommendation Report to be written by SRR Closure and Waste Disposal Authority. Key inputs and assumptions for the modeling were provided to SRNL in SRR-SPT-2011-00113 (2). The table below reiterates the base case and four sensitivity case studies requested in this reference.

Table 1. Case Studies for SDU 6 Modeling

	Baseline Design	Sensitivity Case 1	Sensitivity Case 2	Sensitivity Case 3	Sensitivity Case 4
Tank Diameter	375 ft.				
Tank Height	43 ft.				
Support Columns	208 – 24 in. OD (23 ft. centers)	208 – 24 in. OD (23 ft. centers)	208 – 24 in. OD (23 ft. centers)	208 – 24 in. OD (23 ft. centers)	208 – 24 in. OD (23 ft. centers)
Roof Thickness	7 in.	7 in.	10 in.	7 in.	7 in.
Roof Joints (total linear feet)	2,000 ft.	1,000 ft.	2,000 ft.	2,000 ft.	2,000 ft.
Roof Slope	1.5%	1.5%	1.5%	1.5%	1.5%
Floor Thickness	5 in.	5 in.	5 in.	10 in.	5 in.
Floor Joints (total linear feet)	2,000 ft.	1,000 ft.	2,000 ft.	2,000 ft.	2,000 ft.
Wall Thickness	Tapered 20 in. to 8 in.				
External Curb	N/A	N/A	N/A	N/A	N/A
Base Elevation (bottom floor slab)	270 ft.	270 ft.	270 ft.	270 ft.	250 ft.

3.0 Modeling

3.1 Approach

To satisfy the requirements of the TTR (1), SRNL conducted PORFLOW modeling, that was similar to the modeling performed for Saltstone disposal units in the 2009 PA. In particular, the modeling was based on the Vault 2 Case A analysis performed previously. The modeling assessed the performance of the SDU 6 Baseline design and four sensitivity cases, as shown in Table 1, that varied the disposal unit roof thickness, floor thickness, base elevation, and the total linear feet of roof and floor joints. The total linear feet of roof and floor joints was converted into an equivalent annular region in the PORFLOW model.

The modeling evaluated the potential groundwater contamination from SDU 6. Because these initial scoping calculations were desired quickly and were not intended to be a complete Performance Assessment, the modeling was limited to calculating fluxes to the water table of selected contaminant species for the various design options. This limited analysis provided a comparison of the performance among the design options and a semi-quantitative comparison of SDU 6 performance against that of the Case A Future Disposal Cell (FDC) design analyzed in the 2009 PA (3) and, in particular, a four-pack of FDC vaults which cover approximately the same footprint as the larger SDU 6 vault. Simplifying the analysis to a calculation of fluxes through the vadose zone eliminated the need for aquifer transport calculations and dose calculations which helped to expedite the calculations while still providing a quantitative comparison of the relative performance of the design options. The analysis used the same base case infiltration rates that were used for Case A FDCs in the 2009 PA (3). These infiltration rates reflect the presence of a closure cap that degrades over time. Therefore, no explicit modeling of the closure cover was required. Other key assumptions and approaches used in the modeling are:

- The 2009 PA (3) identifies the key radionuclides contributing to doses from groundwater exposure as: Tc-99, I-129, Np-237, Ra-226 and Pa-231. Parents for Ra-226 and Pa-231 are: U-235, Th-230, U-234 and Pu-238. Based on the results from the 2009 PA modeling, only these five key radionuclides and four parents were used in the analysis.
- The TTR specifically calls for modeling SDU 6 without the presence of a coating on the inner wall to hinder sulfate attack on the concrete. Property degradation curves used in the analysis were modified to model the larger SDU 6 configuration and the absence of a wall coating. It was assumed that the wall degraded to some depth prior to closure from sulfate attack by exposure to saltstone drain water. To simplify the analysis, the lower 41 feet of wall was divided into four equal segments of 10.25 feet each and the upper two feet of wall was modeled as a separate segment. Concrete degradation was applied within each wall segment. The estimate of degradation assumed a uniform one cm of surface cracking and a variable depth of sulfate attack during SDU 6 filling. Drying shrinkage cracks are typically shallow, typically around 1 cm in depth (Levitt 2003, page 5) (4). The depth of sulfate attack was calculated, as outlined in Appendix A, by taking the geometric mean of the minimum (fast reaction) and maximum (slow reaction) penetration depths assuming

an initial concrete saturation of 71.5% which is typical of field exposure conditions (5). Table 2 gives the predicted time for full degradation to occur in the concrete components of the model.

Table 2. Predicted Times to Concrete Failure.

Concrete Section	Years to Fully Degrade
Wall Section 1 (lower section)	80,000
Wall Section 2	60,000
Wall Section 3	40,000
Wall Section 4	25,000
Wall Section 5 (upper section)	16,000
Floor Base Case (5")	8,000
Floor Case 3 (10")	30,000
Roof Base Case (7")	35,000
Roof Case 2 (10")	60,000

- Based on the Vault 2 analysis, the SDU 6 analysis assumed concrete exposure to a sulfate concentration of 0.132 mol/L which was used to estimate concrete degradation as a function of time. Degradation was modeled as an increase in hydraulic conductivity and an increase in effective radionuclide diffusivity which progressed until values similar to those in vadose zone soil were reached.
- A 2.0 inch sheet-drain covering the inner wall of SDU 6 was included in the model. It was assumed that the sheet-drain was filled with saltstone at closure.
- A single 8.0 inch mud mat with properties representative of backfill soil was included as part of the model for future use when these regions may be used to model low quality concrete used as the SDU 6 base material.
- Model features not explicitly defined in SRR-SPT-2011-00113 (2) were taken from the Vault 2 model. For example, as was done for Vault 2, it was assumed that there would be a 2.0 foot thick sand drain over the roof extending 25 feet past the SDU 6 outer wall.
- A 6.0 inch shot-crete region on the SDU 6 outer wall was included in the model but, as was done for Vault 2 modeling, the properties in this region were assumed to be those of backfill soil.
- The roof and floor joints were assumed to be approximately 0.5 mm gaps. As a point of reference, cracks are typically limited to 0.2 mm in watertight structures by design. Because a dimension on the order of 0.5 mm is too small to be included in the model, the joints were modeled as an equivalent 2.0 inch wide annular region containing gravel. The calculation of the equivalent gravel segment is provided in Appendix B. A single annular region with a radius of 318 ft would be located beyond the SDU 6 outer wall. Therefore, three annular regions representing 1000 (159 ft radius), 750 (119 ft radius), and 250 (40 ft radius) linear feet of joints were

created. Sensitivity Case 1 was run by replacing the gravel properties in the two smaller annular regions in the roof and floor with roof and floor concrete properties, respectively.

3.2 Model Description

Model calculations simulating the flow of water infiltration around SDU 6 and radionuclide transport from the disposal unit were made to simulate 15,000 years following placement of a closure cap. Tc-99 transport calculations ran very slowly (because of an additional oxidation sub-model) so these runs were terminated at 12,000 years for purposes of this study. All of the fluid flow and contaminant transport calculations were made using Version 6.30.2 of the PORFLOW code. PORFLOW is a commercial Computational Fluid Dynamics (CFD) code developed by Analytic & Computational Research, Inc.

The Base Case computational model is shown in Figure 1 where areas with different material properties are color coded. Materials corresponding to the figure legend are listed in Table 3. For the base case scenario, the vadose zone is 42 ft deep and the top surface of the model region extends 56.5 ft above ground. This height gives a minimum backfill soil depth of approximately 7.0 ft at the center of the unit. The outer radius of the disposal unit is 188.7 ft and the model domain extends 75.5 ft further to include the 6 inch shot-crete layer, 25 ft sand drain overhang and an additional 50 ft of backfill soil. Some narrow features such as the HDPE-GCL liner above the roof and the joints in the roof and floor are not visible at the scale of Figure 1.

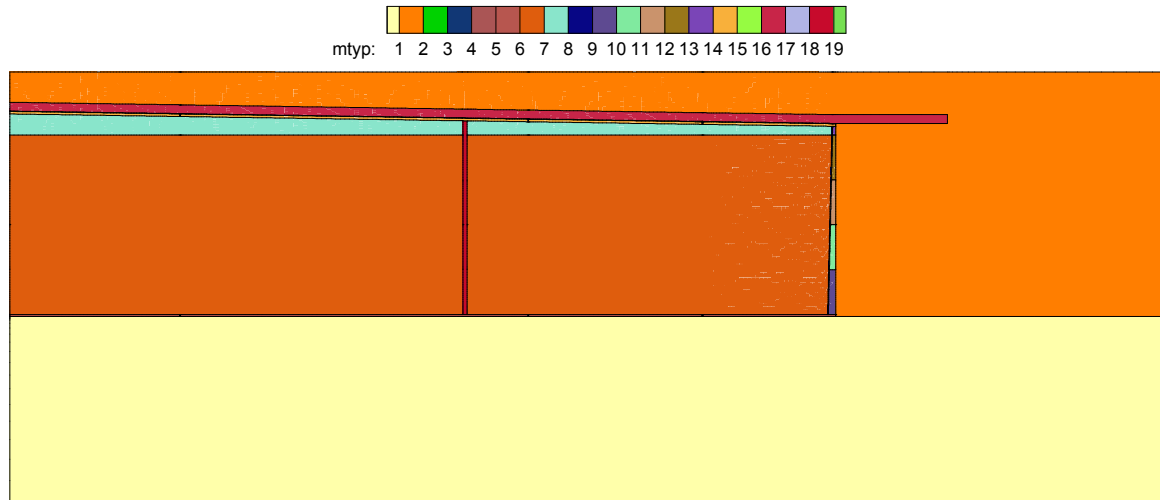


Figure 1. Computational model of SDU6 showing material zones.

Table 3. Materials used in SDU 6 Model.

mtyp	Material	mtyp	Material
1	Native soil in vadose zone	10	Wall section 1
2	Compacted backfill	11	Wall section 2
3	Lower mud mat (unused)	12	Wall section 3
4	Shotcrete (unused)	13	Wall section 4
5	Upper mud mat (unused)	14	Wall section 5
6	Concrete floor	15	Concrete roof
7	Saltstone	16	HDPE GCL over roof
8	Clean grout	17	Sand drain
9	Sheet drain	18	Joint
		19	Concrete support column

3.3 Mesh2d

As shown in Figure 1, the SDU 6 wall thickness varies from 20 inches at the base to eight inches at the top with a slope on the inner surface. The Mesh2d software that has been used to automatically create PORFLOW meshes in previous calculations was not capable of creating a mesh with a vertical slope although horizontally sloped surfaces, such as the SDU 6 roof, could be meshed with the existing Mesh2d code. As an initial task in this project, the Mesh2d code was modified so that it is now capable of meshing both vertical and horizontal sloping surfaces. This modified code is available to modelers for use in future projects.

3.4 Infiltration

Infiltration rates imposed on the upper surface of the model domain were the same as those used in the 2009 Saltstone PA. The infiltration and saturated hydraulic conductivity of selected sections of SDU 6 for the Base Case scenario are plotted in Figure 2.

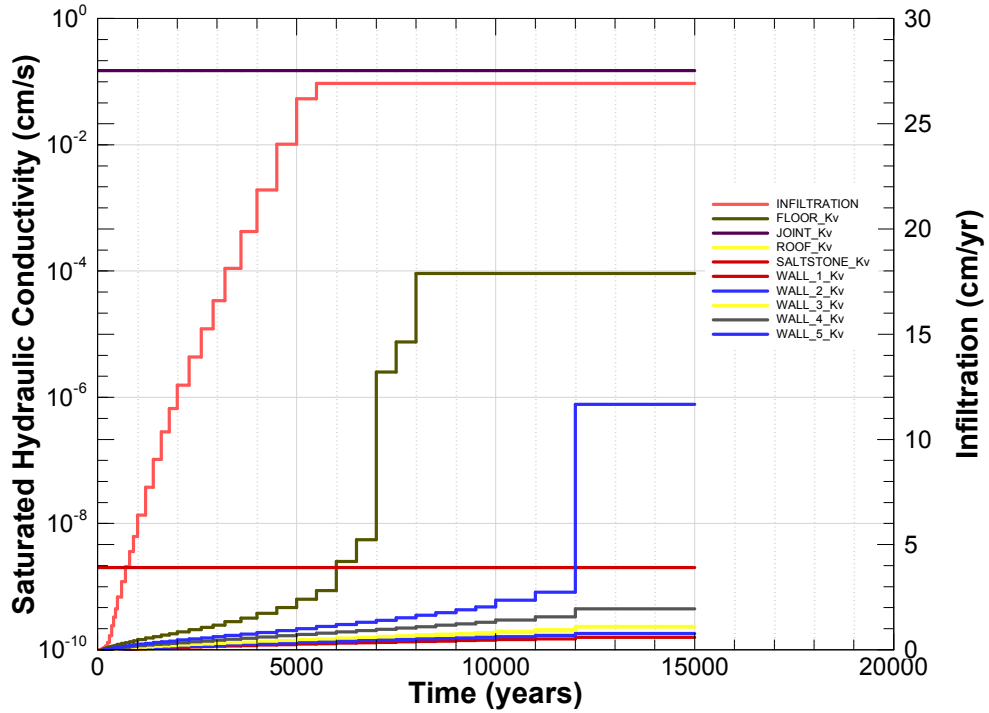


Figure 2. Infiltration and hydraulic conductivity.

4.0 Model Results

Results from the calculations were analyzed to obtain the time history of radionuclide fluxes to the water table. Flux is defined to be the Curies of radionuclide entering the saturated zone per year per Curie of inventory in SDU 6.

4.1 Flow Results

In general, most of the water entering the computational domain was conducted across the disposal unit roof by the sand drain. At the roof edge, the water fell down the wall and at the end of the floor moved horizontally back under SDU 6. A typical result at 500 years into the simulation for the base case is shown in Figure 3 where flow streamlines are plotted over contours of pressure. Figure 3 illustrates flow direction (streamlines) but not the magnitude of the flow. Flow through the saltstone was much less than the water flow along the wall and the return flow under the disposal unit.

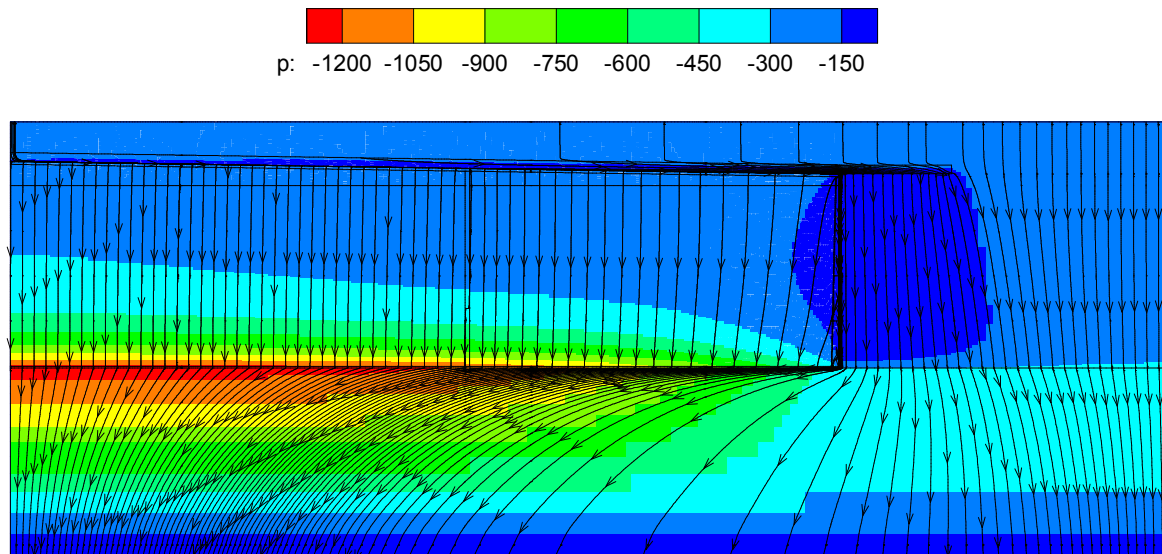


Figure 3. Flow streamlines and pressure contours at 500 years for Base Case calculations.

4.2 Transport Results

Results from the transport calculations showing radionuclide fluxes to the water table for the Base Case and four sensitivity cases and for Vault 2 Case A are plotted in Figures 4 – 12. The Vault 2 Case A calculation exhibits a marked spike in flux at 15,000 years when the hydraulic conductivity of the wall increases significantly due to concrete degradation. Similarly, except for Case 3, the SDU 6 results show a spike in flux at 8,000 years when the five inch floor is fully degraded to vadose zone soil properties.

Ra-226 and I-129 fluxes for SDU 6 and Vault 2 (i.e., species with lower K_d) show the most similar behavior. The SDU 6 model shows higher fluxes initially from water leakage through the floor joints but peak fluxes from SDU 6 for Ra-226 and I-129 are significantly lower than the peaks from Vault 2. For these two radionuclides, Case 3, where the floor

thickness is increased to 10 inches from the Base Case value of five inches, shows a reduced flux which leads to the lowest peak flux of all of the cases.

For the higher K_d species Np-237 and Pa-231 and for Tc-99, the SDU 6 model predicts small but observable initial releases of material through the floor joints, whereas the Vault 2 Case A model predicts essentially no release until around 15,000 years when the vault wall has degraded. For SDU 6 the initial flux levels off within 1,000 to 2,000 years then spikes at 8,000 years when the floor fully degrades. In most cases, the early release of material appears to result in a smaller peak flux than for Vault 2 Case A. With the exception of Ra-226, fluxes to the water table from SDU 6 exceed those from Vault 2 Case A during the 10,000 year assessment period. For Case 3, which increased the floor thickness from five inches to 10 inches, the floor remained intact throughout the simulation which significantly decreased the maximum flux for all radionuclides as expected. The calculations shown in Appendix C verified that the origin of the initial fluxes was flow through the floor joints.

For the SDU 6 design, the Base case, Case 1 (50% less joint length) and Case 2 (10 inch vs seven inch roof) all gave very similar results. The modeling approach may not have been able to distinguish between the difference in joint length. As noted in Section 3.1, the joints were modeled using three 2-inch thick annular rings of gravel. The outer ring represented half of the joint area. Since Case 1 specified using half the joint area, this was accomplished by changing the material properties of the inner and middle roof and floor joint annuli from gravel to those of roof and floor concrete, respectively. However, as Figure 3 shows, lateral flow under the floor is much stronger at the outer joint position than at the inner two positions. This may have contributed to the very small difference from Base Case results found for Case 1. Nevertheless, it does not appear that increasing the roof thickness by 50% or a 50% decrease in joint length will have a significant impact on releases from SDU 6.

As expected, Case 4, which reduced the distance from the SDU 6 floor bottom to the water table by 20 ft, resulted in a higher fluxes for all radionuclides. For Ra-226, the increase in flux was approximately a factor of two and less for the other radionuclides except for I-129 where only a small increase was observed.

Peak fluxes and the years when they occur are tabulated for the SDU 6 Base Case and Vault 2 Case A in Table 4 and for the SDU 6 sensitivity cases in Table 5. Peak fluxes during the 10,000 year period of analysis and at any time during the simulation are listed.

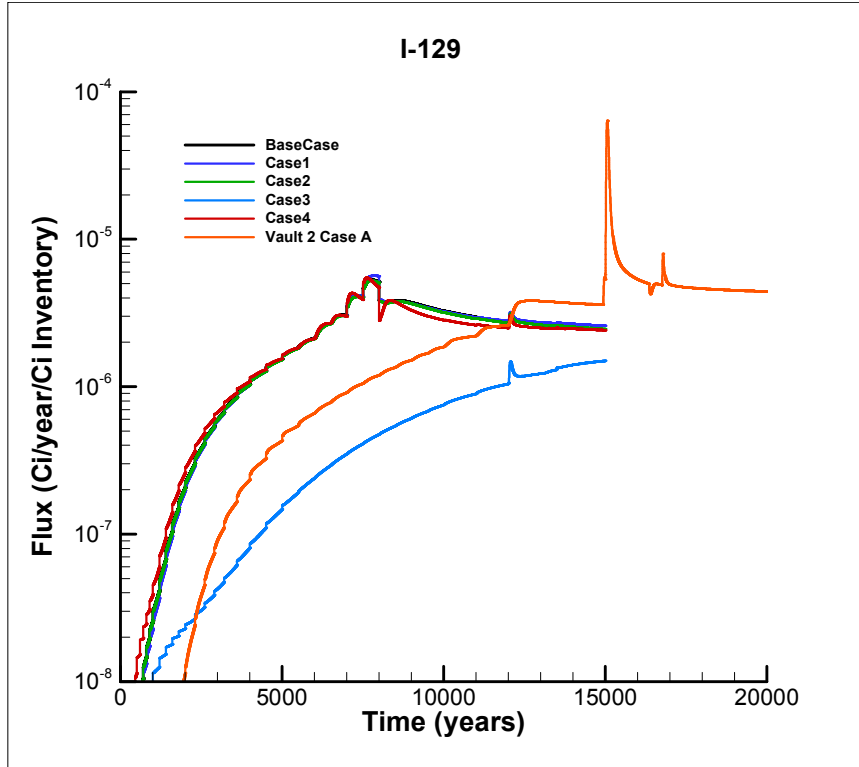


Figure 4. Flux to water table of I-129 from SDU 6.

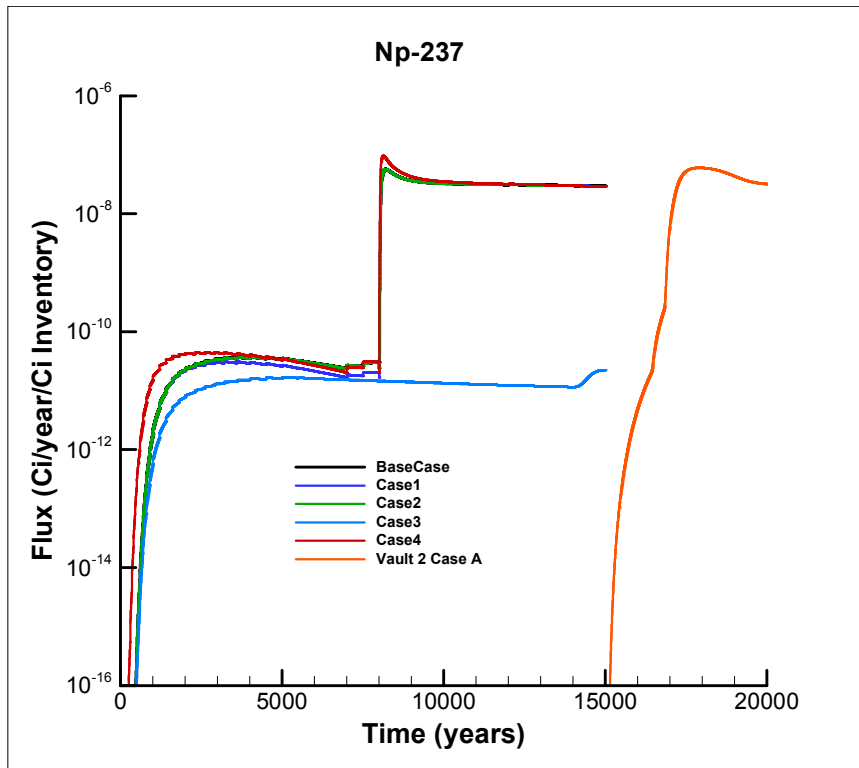


Figure 5. Flux to water table of Np-237 from SDU 6.

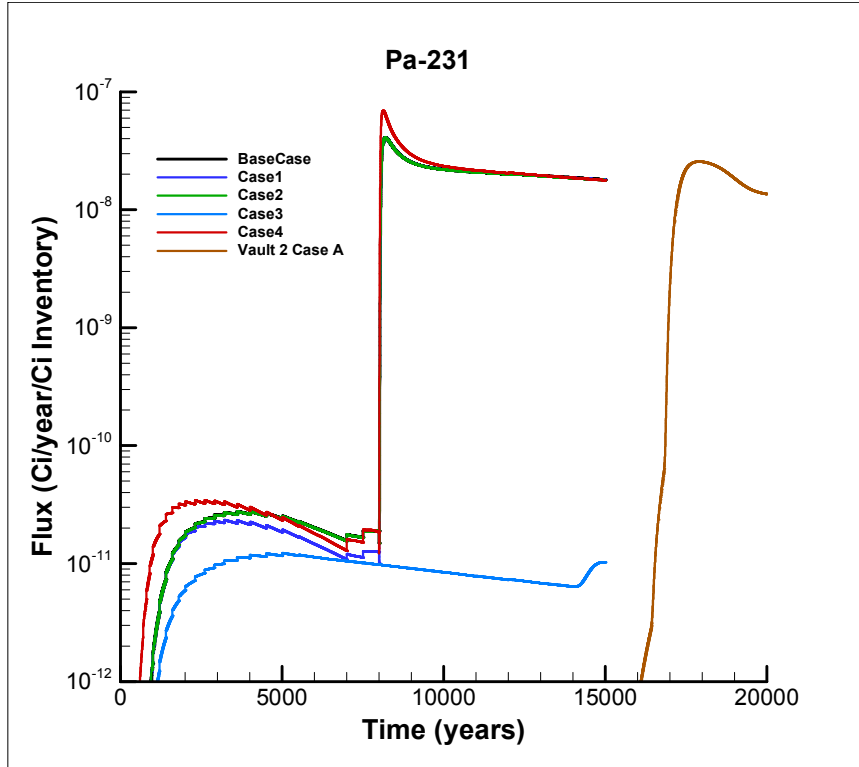


Figure 6. Flux to water table of Pa-231 from SDU 6.

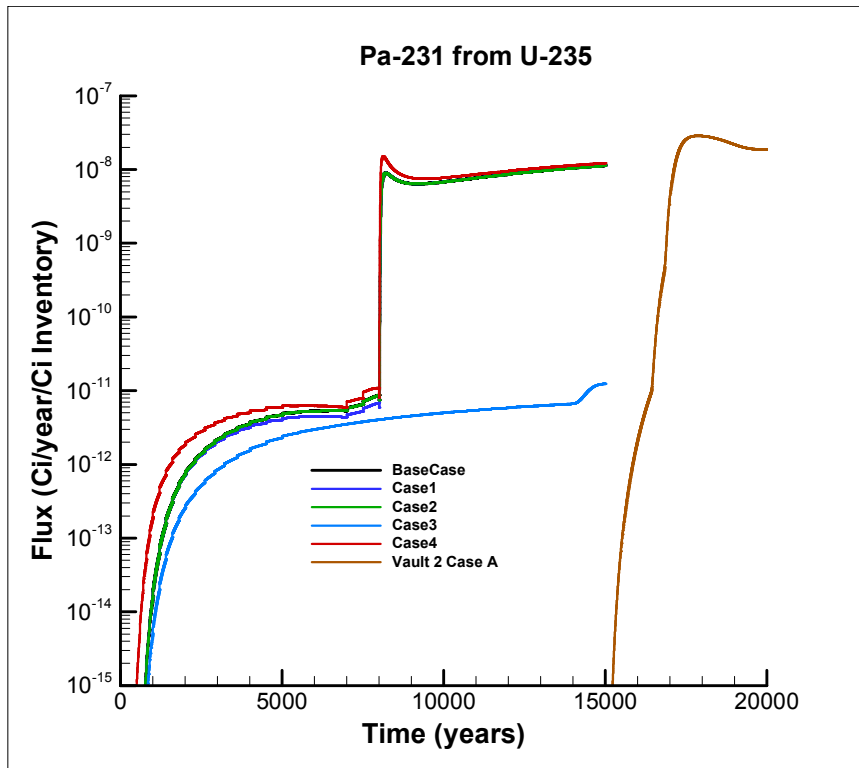


Figure 7. Flux to water table of Pa-231 as daughter of U-235 from SDU6.

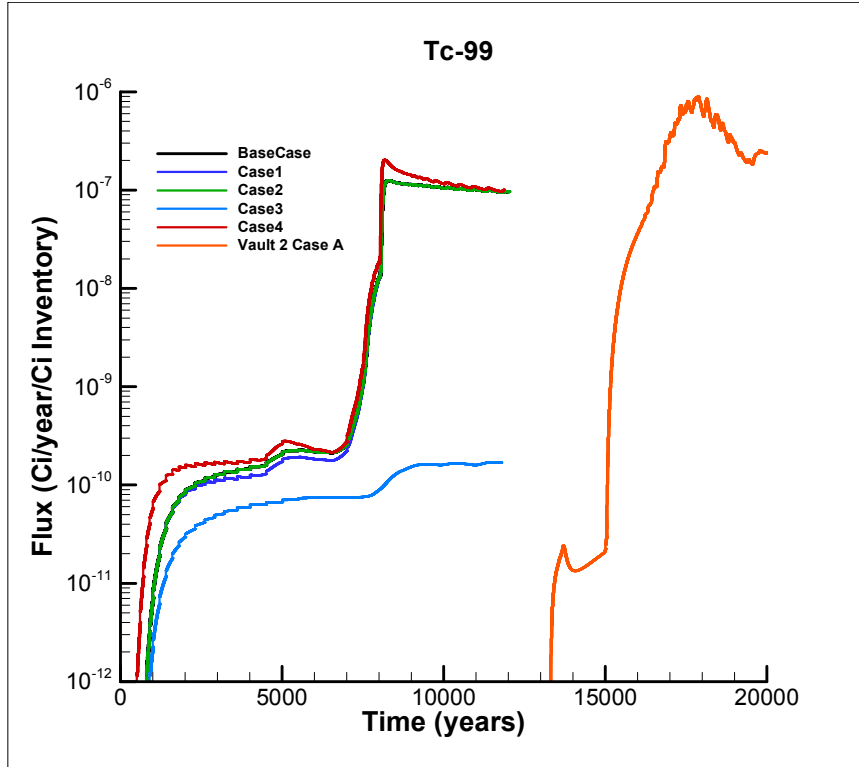


Figure 8. Flux to water table of Tc-99 from SDU 6.

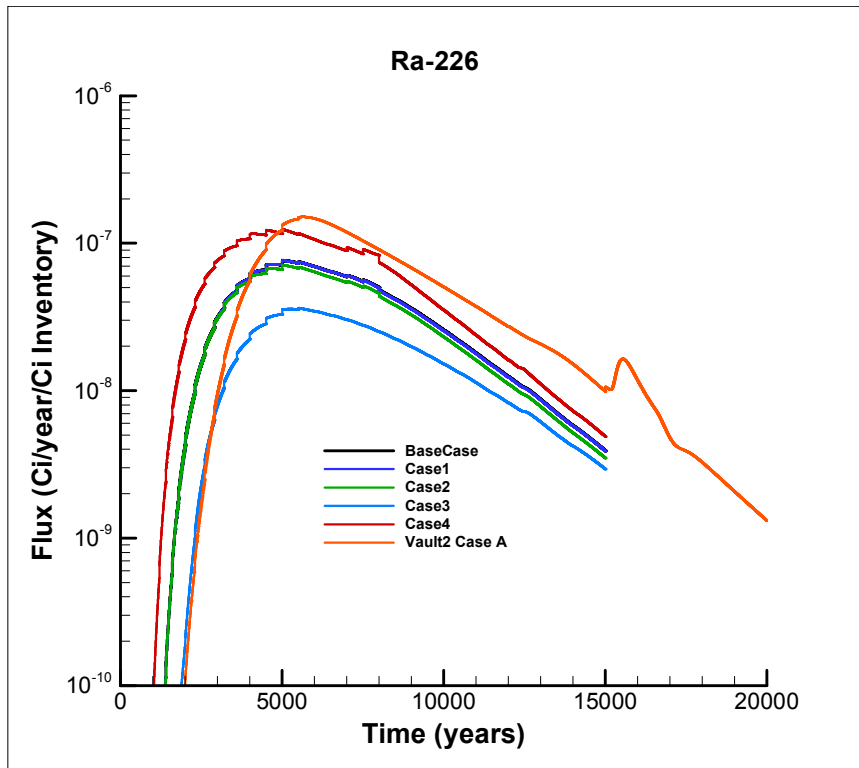


Figure 9. Flux to water table of Ra-226 as parent from SDU 6.

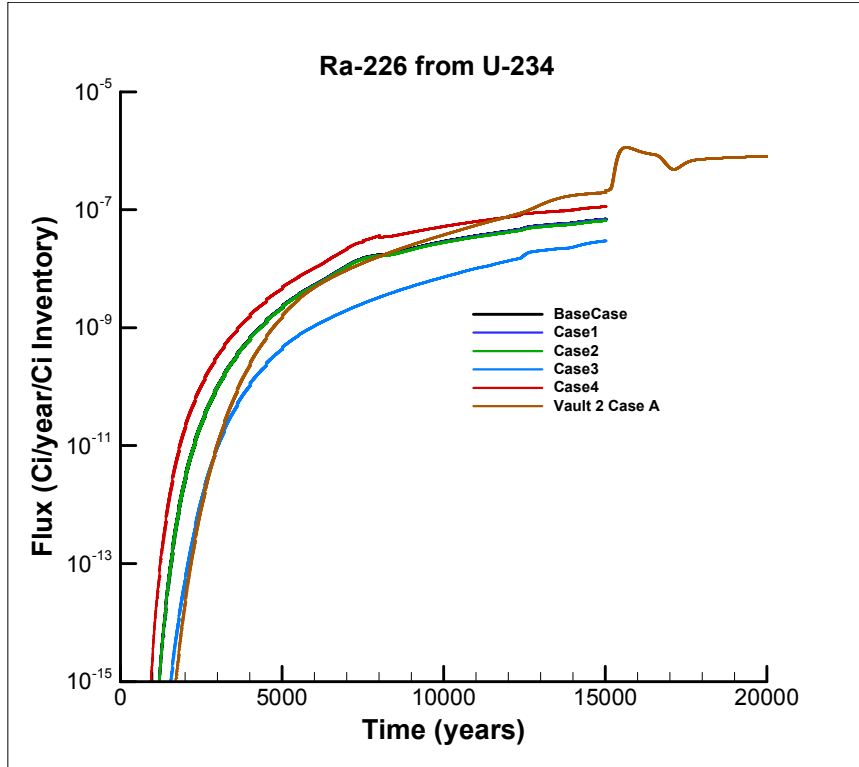


Figure 10. Flux to water table of Ra-226 as daughter of U-234 from SDU 6.

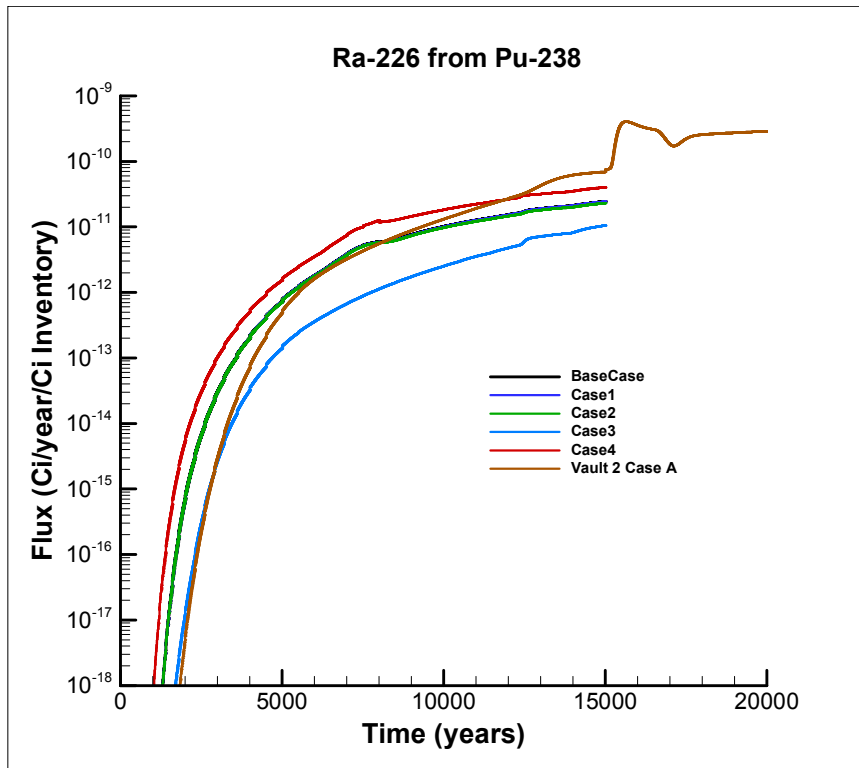


Figure 11. Flux to water table of Ra-226 as daughter of Pu-238 from SDU 6.

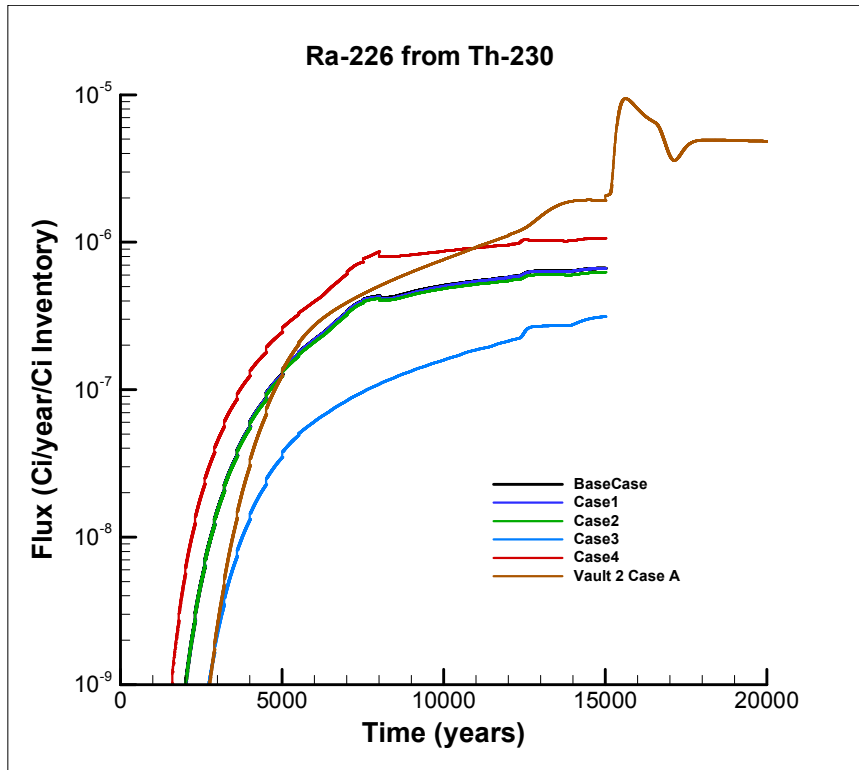


Figure 12. Flux to water table of Ra-226 as daughter of Th-230 from SDU 6.

Table 4. Peak Flux to Water Table and Year of Occurrence for SDU 6 Base Case and Vault 2 Case A

	Radionuclide	Within 10,000 year period of analysis		At any time during analysis	
		Peak Flux (Ci/yr/Ci)	Year	Peak Flux (Ci/yr/Ci)	Year
SDU 6	I-129	5.29E-06	7737	5.29E-06	7738
	Tc-99	1.25E-07	8278	1.25E-07	8278
	Np-237	5.70E-08	8183	5.70E-08	8184
	Ra-226	7.64E-08	5001	7.64E-08	5002
	Pa-231	4.09E-08	8180	4.09E-08	8181
	Ra-226 (U-234)	1.88E-10	9999	4.48E-10	14999
	Pa-231 (U-235)	4.19E-13	8185	5.30E-13	14992
	Ra-226 (Pu-238)	1.84E-10	10000	4.43E-10	14996
	Ra-226 (Th-230)	1.08E-08	10000	1.41E-08	15000
Vault 2 Case A	I-129	1.86E-06	10000	6.37E-05	15063
	Tc-99	6.79E-15	10000	9.02E-07	17865
	Np-237	1.24E-22	10000	6.01E-08	17873
	Ra-226	1.51E-07	5618	1.51E-07	5619
	Pa-231	1.27E-23	10000	2.56E-08	17871
	Ra-226 (U-234)	2.46E-10	10000	7.43E-09	15626
	Pa-231 (U-235)	1.02E-25	10000	1.33E-12	17830
	Ra-226 (Pu-238)	2.40E-10	10000	7.37E-09	15631
	Ra-226 (Th-230)	1.62E-08	10000	2.00E-07	15611

Table 5. Peak Flux to Water Table and Year of Occurrence for SDU 6 Sensitivity Cases.

	Radionuclide	Within 10,000 year period of analysis		At any time during analysis	
		Peak Flux (Ci/yr/Ci)	Year	Peak Flux (Ci/yr/Ci)	Year
Case 1	I-129	5.66E-06	7843	5.66E-06	7844
	Tc-99	1.25E-07	8282	1.25E-07	8282
	Np-237	5.69E-08	8181	5.69E-08	8182
	Ra-226	7.63E-08	5001	7.63E-08	5002
	Pa-231	4.09E-08	8183	4.09E-08	8180
	Ra-226 (U-234)	1.87E-10	10000	4.48E-10	15000
	Pa-231 (U-235)	4.19E-13	8185	5.28E-13	14990
	Ra-226 (Pu-238)	1.83E-10	10000	4.43E-10	15000
	Ra-226 (Th-230)	1.07E-08	9999	1.41E-08	14981
Case 2	I-129	5.24E-06	7738	5.24E-06	7739
	Tc-99	1.25E-07	8276	1.25E-07	8276
	Np-237	5.69E-08	8185	5.69E-08	8186
	Ra-226	7.11E-08	5001	7.11E-08	5002
	Pa-231	4.09E-08	8180	4.09E-08	8181
	Ra-226 (U-234)	1.82E-10	10000	4.25E-10	14997
	Pa-231 (U-235)	4.18E-13	8186	5.26E-13	14997
	Ra-226 (Pu-238)	1.78E-10	10000	4.20E-10	14998
	Ra-226 (Th-230)	1.03E-08	9997	1.33E-08	14978
Case 3	I-129	7.53E-07	10000	1.50E-06	14998
	Tc-99	1.63E-10	9500	1.71E-10	11506
	Np-237	1.70E-11	5001	2.22E-11	14932
	Ra-226	3.63E-08	5501	3.63E-08	5502
	Pa-231	1.23E-11	5001	1.23E-11	5002
	Ra-226 (U-234)	4.72E-11	10000	1.94E-10	14998
	Pa-231 (U-235)	2.33E-16	9999	5.73E-16	14934
	Ra-226 (Pu-238)	4.60E-11	9999	1.91E-10	15000
	Ra-226 (Th-230)	3.38E-09	10000	6.65E-09	14999
Case 4	I-129	5.49E-06	7605	5.49E-06	7606
	Tc-99	2.03E-07	8159	2.03E-07	8159
	Np-237	9.59E-08	8119	9.59E-08	8120
	Ra-226	1.24E-07	5001	1.24E-07	5002
	Pa-231	6.91E-08	8117	6.91E-08	8118
	Ra-226 (U-234)	3.40E-10	10000	7.39E-10	15000
	Pa-231 (U-235)	7.04E-13	8117	7.04E-13	8118
	Ra-226 (Pu-238)	3.34E-10	10000	7.31E-10	14995
	Ra-226 (Th-230)	1.84E-08	9996	2.26E-08	14924

5.0 Conclusions

In general, as shown in Table 4, when compared to Vault 2 Case A, the Base Case SDU 6 design produced higher peak fluxes to the water table during the 10,000 year period of analysis but lower peak fluxes within a 15,000 to 20,000 time frame. SDU 6 will contain approximately ten times the inventory of a single Vault 2 and the SDU 6 footprint is comparable to that of a group of four Vault 2 disposal units. Therefore, the radionuclide flux from SDU 6 and that from a single Vault 2 are not directly comparable. A more direct comparison would be to compare the maximum dose obtained at the 100 m boundary from the seven SDU's that will replace the 64 FDC's analyzed in the 2009 PA. This analysis will be performed in the next set of calculations planned for SDU design evaluation. Aquifer transport and dose calculations were not intended to be part of this initial scoping study. However, results from this study do indicate that replacement of the FDC design with SDU would not yield significantly higher peak doses. If the thickness of the SDU 6 floor is increased, peak doses would not occur during the 10,000 year period of analysis.

5.1 Model Improvements

During review of the modeling results, several minor improvements to the modeling strategy were identified. These improvements will be applied in future modeling with the SDU 6 design and are described below.

1. **Soil Depth above SDU 6** – For all calculations, the above ground height of the model was kept at the fixed value of 56.5 feet which placed 6.92 feet of soil over SDU 6 at the center of the unit. However, for Case 2, where the roof thickness was increased from 7 inches to 10 inches, and Case 3, where the floor thickness was increased from 5 inches to 10 inches, the above ground height was not adjusted as was intended. Therefore, for Case 2, the backfill was 0.25 foot thinner than for the Base Case and 0.42 foot thinner for Case 3. It was judged that these differences would have an insignificant impact on these scoping results. For the next set of calculations, the minimum soil depth above SDU 6 will be set to 7.0 feet for all cases.
2. **Wall Base Joint** – While the model included a treatment of the cement joints in the roof and floor, joints between the wall and floor and between the wall and roof were not included in the model. The base joint between the wall and floor is a two inch footing which could conservatively be modeled as two inches of gravel between the base of the wall and the floor. The roof joint could also be modeled as a two inch space filled with gravel. Because the joints in the wall and floor concrete were modeled as two inch gravel gaps, which is likely conservative, and no credit was taken for mud mats below the floor in the model, it was concluded that water flow was adequately modeled for the purpose of comparing design alternatives and no additional calculations were necessary. The final SDU 6 model will include the joints between the wall and floor and between the wall and roof.

3. **Concrete Degradation** – Appendix A explains the calculation that was used to estimate initial concrete degradation in the SDU 6 wall segments. In the next stage of modeling, degradation of the upper 2.0 ft of wall will be neglected (since it is not exposed to sulfate attack) and the estimate of wall degradation in the lower 41 ft of wall will be reexamined. This change is again not expected to significantly impact model results because the SDU 6 wall did not fully degrade throughout the duration of the model calculations. Also, the floor will be subjected to early degradation from sulfate attack because like the wall it lacks a short-term interior waterproof coating.
4. **Computational Mesh** – The computational mesh at the interface between the end of the sand drain and the last radial segment may not be optimal because a small cell was placed adjacent to a large one. A preliminary test calculation indicated that refining the mesh did not improve convergence or change results. Additional efforts will be made to refine the mesh in the next phase of SDU modeling.
5. **Computational Speed** – Flow solutions at times greater than about 10,000 years proceeded very slowly as did transport calculations for Tc-99. Additional effort will be made to improve model numerical behavior during the next series of calculations.

6.0 References

1. Rosenberger, K. H., “SDU-6 Scoping Modeling”, Task Technical Request, HLW-SSF-TTR-2012-0017, Rev. 0, January 25, 2011.
2. Clendenen, G. B., “SDU-6 Performance Assessment Initial Modeling Inputs”, SRR-SPT-2011-00113, Rev. 0, November 29, 2011.
3. “Performance Assessment for the Saltstone Disposal Facility at the Savannah River Site”, SRR-CWDA-2009-00017, Rev. 0, October, 2009.
4. Levitt, M. "Concrete Materials: Problems and Solutions." Taylor & Francis e-Library. 2003.
5. Sappington, F. C., and M. A. Phifer. "Moisture Content and Porosity of Concrete Rubble Study." WSRC-TR-2005-00054, Revision 0. October 2005.

Appendix A Estimation of Initial Wall Degradation

Degradation of the concrete wall from sulfate attack immediately after exposure of the concrete to saltstone drain water can be approximately bounded by two scenarios defined by the rate of chemical reaction compared to capillary liquid transport.

If dissolved sulfate reacts with concrete minerals much faster than the transport rate, then sulfate cannot advance past the reaction front until all of the local reaction capacity is consumed. Damage front penetration will be controlled by the amount of bleedwater (and sulfate) imbibed and the reaction capacity of the concrete minerals. The penetration depth for this fast reaction scenario is calculated using the formula:

$$x_1 = \frac{\varphi \delta s L C}{R}$$

where: x_1 degraded concrete length (same units as L)
 φ concrete porosity (0.11),
 δs change in concrete saturation from the assumed initial value of 0.715 to full saturation (0.285),
 L thickness of concrete (units of length),
 C sulfate concentration (0.15 mol/L), and
 R reaction capacity of the concrete (1.77 mol/L)

The initial saturation value is typical of field exposure conditions (WSRC-TR-2005-00054, Rev. 0). The reaction capacity is derived from Equation (9) of SRNL-STI-2009-00115 Rev. 1. Values of the degraded concrete calculated using this equation proved to be very small, less than 0.05 inches.

If the reaction rate is slow of the other hand, then sulfate will advance as far as the wetting front before reacting with solids and partially consuming the reaction capacity. An upper bound on the degradation from sulfate attack was estimated by assuming that all of the concrete exposed to imbibed bleedwater under this scenario will be damaged:

$$x_2 = \varphi \delta s L$$

This slow reaction analysis produced damage penetration depths ranging from 2.4 to 5.3 inches depending on the thickness of the wall segment, roughly two orders of magnitude larger than the fast reaction scenario.

Considering this large difference in magnitude, representative blended values for sulfate attack degradation were then obtained by taking the geometric average of x_1 and x_2 :

$$x_{avg} = \sqrt{x_1 x_2}$$

This intermediate estimate of the concrete degradation from sulfate attack was then about 0.2 to 0.5 inches and was the same order of magnitude as the assumed 1.0 cm (0.4 in) surface cracking. Adding the two values was used as an estimate of the total concrete degradation at the start of the analysis. Calculated penetration depths are provided in Table

A.1 below. The degradation was also applied to Wall Section 5 which is the two foot upper section in contact with clean grout. A more consistent approach would have been to not apply the sulfate attack degradation in Section 5 and this approach will be adopted in future modeling.

Table A.1 Estimation of Concrete Degradation Length

Wall Segment	Average Thickness (inches)	crack (inches)	x_1 (inches)	x_2 (inches)	x_{avg} (inches)	x_{total} (inches)
1	18.57	0.394	0.049	5.29	0.511	0.904
2	15.71	0.394	0.042	4.48	0.432	0.826
3	12.85	0.394	0.034	3.66	0.354	0.747
4	9.99	0.394	0.027	2.85	0.275	0.668
5	8.38	0.394	0.022	2.36	0.228	0.621

Appendix B Equivalent Gravel Flow Path for Roof and Floor Joints

Joints in the roof and floor of SDU 6 are assumed to be 0.455 mm gaps between the concrete slabs. Watertight structures are designed to have cracks of less than 0.2 mm and the SDU joints will have water-stops installed. The assumption of a 0.455 mm gap, which, as shown below, is equivalent to 2.0 inches of gravel, appears to be reasonable and is made to obtain a convenient model dimension. If a better basis for the assumed gap size can be established, it will be applied in future analysis.

The saturated hydraulic conductivity for an aperture of width x is given by:

$$K_{sat} = \frac{\rho g x^2}{12 \eta}$$

where: xaperture width (m)
 g gravitational constant, 9.81 (m/s²)
 ρ density of water, 998 (kg/m³)
 η viscosity of water, 0.001002 (kg/m-s)

For a 0.455 mm aperture, this equation gives a saturated conductivity of 0.169 m/s.

Gravel has a saturated conductivity of 0.15 cm/s. Therefore, the equivalent gravel width for a 0.455 mm aperture would be:

$$b (0.0015 \text{ m/s}) = (0.455 \text{ mm})(0.169 \text{ m/s})$$

Which gives an equivalent gravel width of 51.3 mm or 2.0 inches. Obviously, the choice of a 0.455 mm gap was made to produce a convenient 2.0 inch equivalent gravel width. While the aperture width of approximately 0.5 mm does not seem unreasonable, as mentioned above, this assumption was made for convenience and is not based on any physical evidence.

Appendix C Model Runs Without Roof and Floor Joints

A set of calculations was made to verify that the origin of the initial fluxes observed for Np-237, Pa-231 and Tc-99 in the SDU 6 design but not seen in the previous Vault 2 PA calculations was flow through the floor joints. These calculations were made by replacing the material in the gravel joint gaps in the roof and floor with roof and floor cement, respectively. Results from these calculations are shown for Np-237, Pa-231, Tc-99 and Ra-226 in Figures C1 through C4, respectively. The figures compare fluxes calculated for the SDU 6 Base Case with and without roof and floor joints to fluxes calculated for Vault 2 Case A in the 2009 Saltstone PA. It can be seen that, without the roof and floor joints, the SDU 6 fluxes show the same pattern as found for Vault 2 with negligible releases of high Kd species until a concrete component of the vault fails. For Ra-226, there is almost no difference between the fluxes with and without roof and floor joints. As seen in the previous Vault 2 calculations, low Kd species have significant releases early in the simulations.

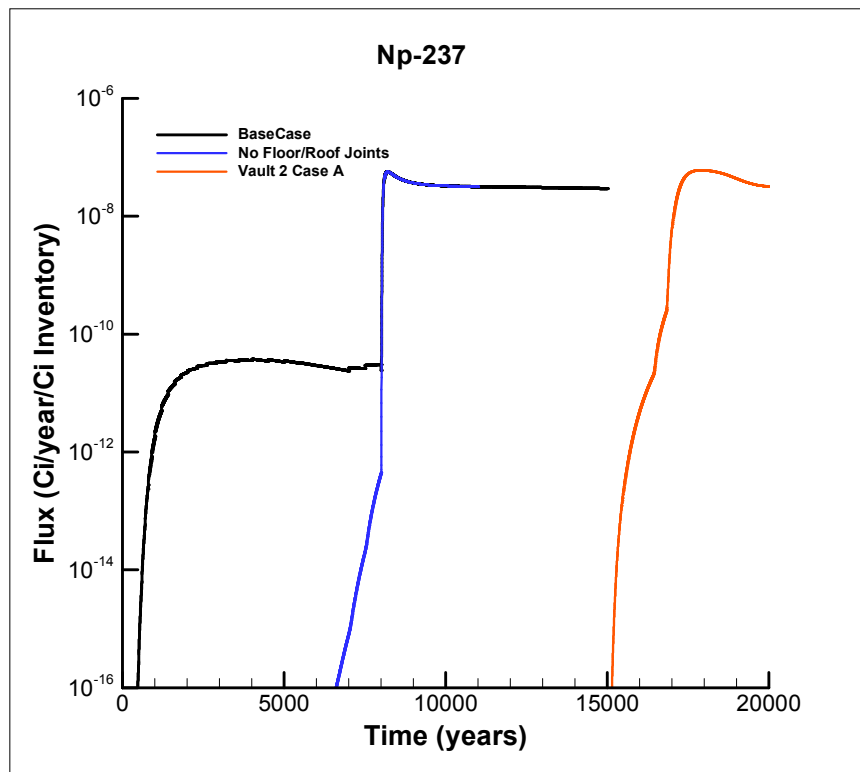


Figure C1. Flux to water table of Np-237 from SDU 6 with and without roof and floor joints compared to flux from Vault 2.

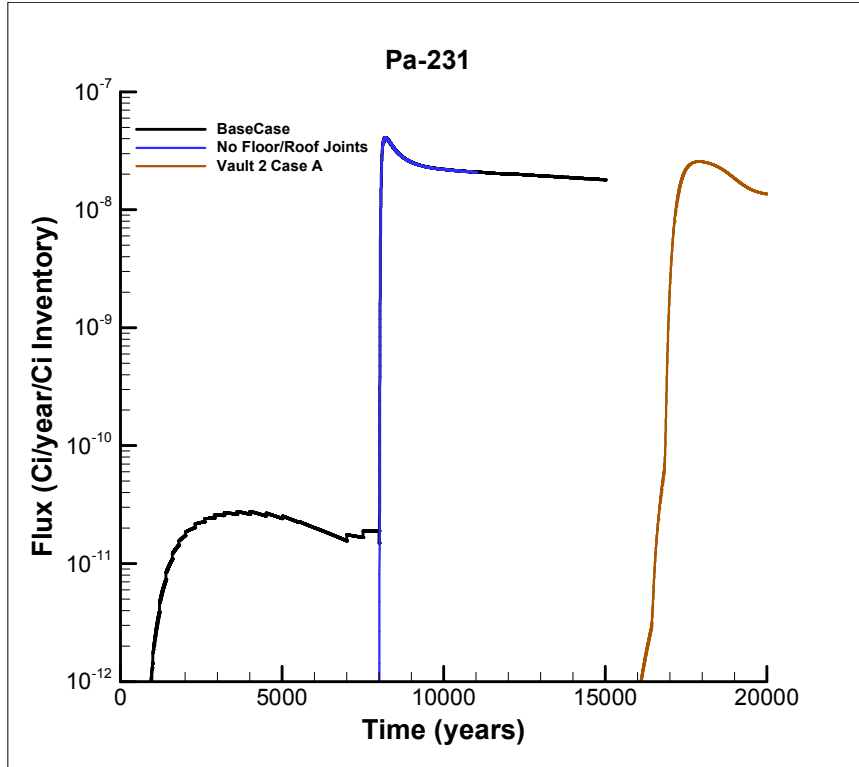


Figure C2. Flux to water table of Pa-231 from SDU 6 with and without roof and floor joints compared to flux from Vault 2.

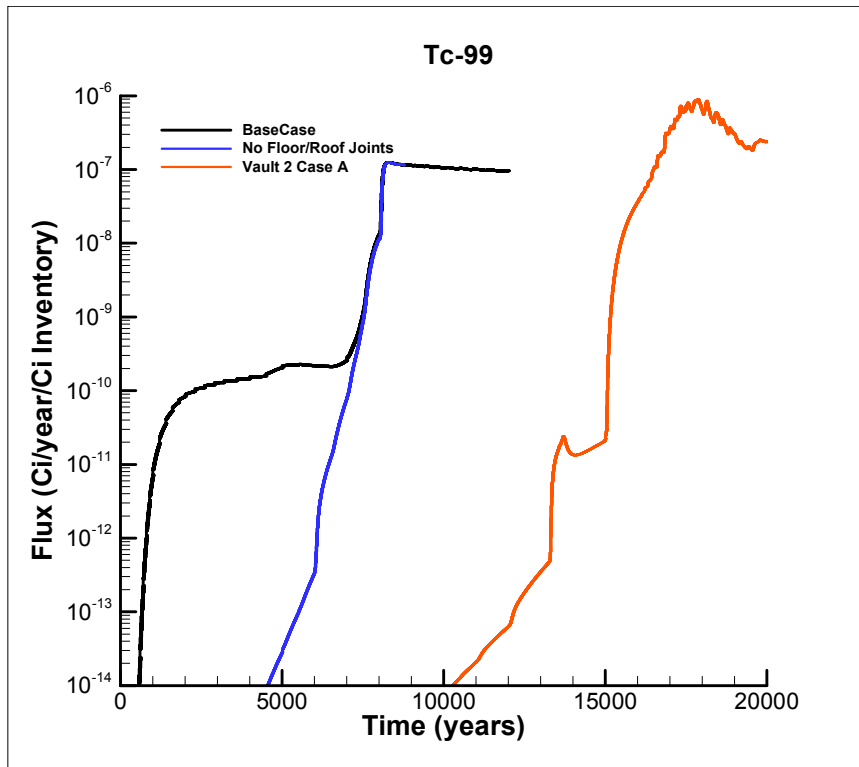


Figure C3. Flux to water table of Tc-99 from SDU 6 with and without roof and floor joints compared to flux from Vault 2.

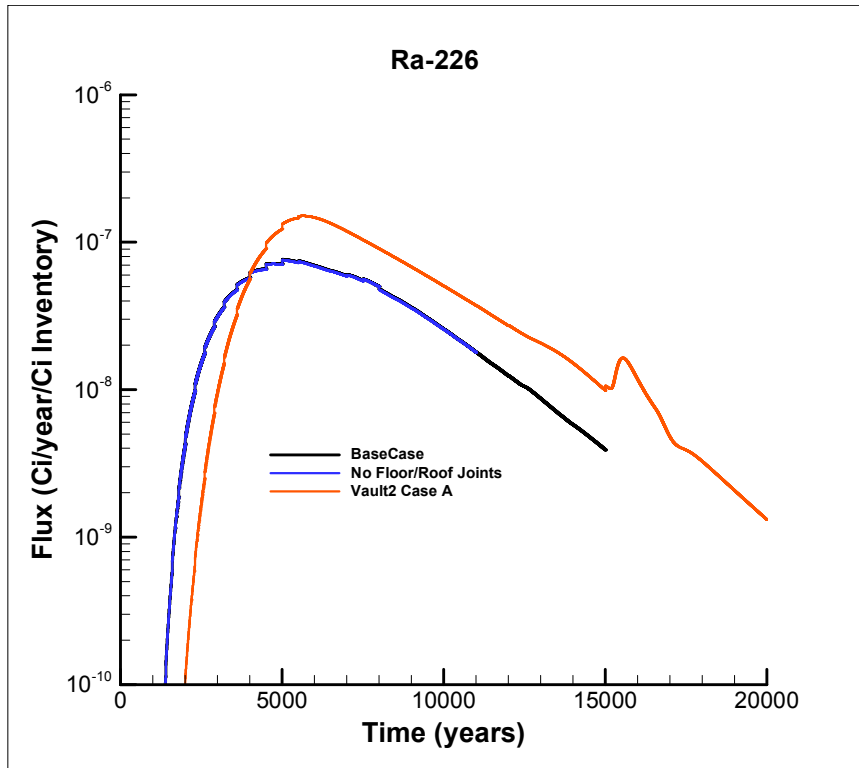


Figure C4. Flux to water table of Ra-226 from SDU 6 with and without roof and floor joints compared to flux from Vault 2.

Appendix D Design Check Documentation

Design Check Instructions for SDU 6 PORFLOW Calculations

1.0 Background

The five case studies shown in Table 1 below will be run for the SDU 6 analysis. Differences between the baseline design and sensitivity cases are highlighted in the table. Files for each case study will be stored in main directory [\\godzilla-01\hpc_project\projwork54\megatank\smith\SDU6](#) in the subdirectories shown on the second line of Table 1.

Table 1. Case Studies for SDU 6 Modeling

	Baseline Design	Sensitivity Case 1	Sensitivity Case 2	Sensitivity Case 3	Sensitivity Case 4
File Directory	\VadoseBaseCase	\VadoseCase1	\VadoseCase2	\VadoseCase3	\VadoseCase4
Tank Diameter	375 ft.				
Tank Height	43 ft.				
Support Columns	208 – 24 in. OD (23 ft. centers)	208 – 24 in. OD (23 ft. centers)	208 – 24 in. OD (23 ft. centers)	208 – 24 in. OD (23 ft. centers)	208 – 24 in. OD (23 ft. centers)
Roof Thickness	7 in.	7 in.	10 in.	7 in.	7 in.
Roof Joints (total linear feet)	2,000 ft.	1,000 ft.	2,000 ft.	2,000 ft.	2,000 ft.
Roof Slope	1.5%	1.5%	1.5%	1.5%	1.5%
Floor Thickness	5 in.	5 in.	5 in.	10 in.	5 in.
Floor Joints (total linear feet)	2,000 ft.	1,000 ft.	2,000 ft.	2,000 ft.	2,000 ft.
Wall Thickness	Tapered 20 in. to 8 in.				
External Curb	N/A	N/A	N/A	N/A	N/A
Base Elevation (bottom floor slab)	270 ft.	270 ft.	270 ft.	270 ft.	250 ft.

To verify that the PORFLOW calculations are performed correctly the following four general areas require design checking:

Area	Design Check
Material Properties	Greg Flach
Computational Mesh	Thong Hang
PORFLOW Flow Calculations	Thong Hang
PORFLOW Transport Calculations	Thong Hang

2.0 Material Properties

The basic material property files are located in directory: [\\godzilla-01\hpc_project\projwork54\megatank\smith\SDU6\Common](#). The following checks need to be performed:

1. Check that the concrete degradation calculations in Excel workbook CementitiousMaterialDegradation.xls are correct.
2. Verify that the factors calculated in the spreadsheet have been entered into Excel workbook MaterialFactor1.xls correctly.
3. Verify that the entries in Excel workbook MaterialFactor2.xls are correct.
4. Verify that the entries in Excel workbook MaterialZones.xls are correct.
5. Verify that the entries in Excel workbook MaterialPalette.xls are correct.

Response from Greg Flach

Frank,

As proposed in the design check instructions, I checked the material property assignments and material degradation calculations for the SDU-6 PORFLOW simulations. All technical issues have been satisfactorily resolved. I have also reviewed the technical report and am ready to approve it.

Greg Flach
 Savannah River National Laboratory
 773-42A, Savannah River Site, Aiken, SC 29808
 803-725-5195
 gregory.flach@srnl.doe.gov

3.0 Computational Mesh

The mesh is computed for each case as part of preprocessing for PORFLOW flow calculations. The geometries for each case were first calculated in Excel workbook Mesh_Geometry_Rev0.xls in directory [\\godzilla-01\hpc_project\projwork54\megatank\fsmith\SDU6\geometry\Analysis](#). Input and output files for the mesh generation and material property assignments are located in the \Flow subdirectories of the case file directories listed in Table 1. For each case, the following checks need to be performed:

1. Verify that the calculations in Mesh_Geometry_Rev0.xls correctly represent the SDU 6 geometry.

Under the “radial” tab, “Column Annulus” value (N7) is given in inches, but the ft-to-cm conversion factor (M7) is specified.

As you found, this error was corrected in the actual mesh files used in the calculations. I have changed the spreadsheet to be consistent with the actual mesh used to avoid any errors in the future.

	A	B	C	D	E	F	G	H	I	J	K	L	M	N	O	P	Q	R
1		Average Width																
2							Location					iFlag	scale	dx/x			width	
3		Zone	True Value	As Modeled	conversion unit		in	ft	cm	position		1	2.54	0			0	
4		Inner Joint	38.789	38.789	ft		465.46	38.79	1182.28	absolute	1	30.48	38.79				1182.28	
5		Inner Joint Annulus	2.0	2.0	in		2.00	0.17	5.08	add	0	2.54	2.00				1187.36	
6		Column	103.500	103.500	ft		1242.00	103.50	3154.68	absolute	1	30.48	103.50				3154.68	
7		Column Annulus	1.0	1.0	ft		12.00	1.00	30.48	add	0	30.48	12.00				3520.44	
8		Middle Joint	118.366	118.366	ft		1420.39	118.37	3607.80	absolute	1	30.48	118.37				3607.80	
9		Middle Joint Annulus	2.0	2.0	in		2.00	0.17	5.08	add	0	2.54	2.00				3612.88	
10		Outer Joint	158.155	158.155	ft		1897.86	158.15	4820.56	absolute	1	30.48	158.15				4820.56	
11		Outer Joint Annulus	2.0	2.0	in		2.00	0.17	5.08	add	0	2.54	2.00				4825.64	
12		Sheet Drain (mid point)	187.333	187.333	ft		2248.00	187.33	5709.92	variable position	5	30.48	187.33				5709.92	
13		Inner Wall	2.0	2.0	in		2.00	0.17	5.08	add	0	2.54	2.00				5715.00	
14		Outer Wall	188.667	188.667	ft		2264.00	188.67	5750.56	absolute	1	30.48	188.67				5750.56	
15		Shotcrete	6.0	6.0	in		6.00	0.50	15.24	add	0	2.54	6.00				5765.80	
16		Extent of Sand Drain	25.0	25.0	ft		300.00	25.00	762.00	add	0	30.48	25.00				6527.80	
17		Extent of Model	50.0	50.0	ft		600.00	50.00	1524.00	add	0	30.48	50.00				8051.80	
18																		264.167 ft

- Verify that the data in xMesh.dat, yMesh.dat and mtypMesh.dat files in the \Flow subdirectories for each case is correct (i.e. corresponds to the geometry calculation).

xMesh.dat: What is iFlag of 5 (not defined)?

The first task I performed on this project was to modify the Mesh2d code to allow us to model the sloped wall in SDU 6. iFlag5 tells the code that the next data entries are a series of (in this case 6) points defining (in this case radial) zone vertices at the indicated (in this case axial) zones.

xMesh.dat for Base Case was checked against *Mesh_Geometry_Rev0.xls*. Note that although wrong conversion factor was used for “Column Annulus” in *Mesh_Geometry_Rev0.xls*, correct conversion factor was applied in *xMesh.dat*. *xMesh.dat* correctly reflects data specified in *Mesh_Geometry_Rev0.xls*. *xMesh.dat* for all other cases were then compared with the Base Case *xMesh.dat*. They are identical as expected.

Likewise, *yMesh.dat* for Base Case was found to correctly reflect data specified in *Mesh_Geometry_Rev0.xls*. *yMesh.dat* for all other cases were compared with the Base Case *xMesh.dat*. The results are given below:

Base Case vs. Case 1

```
Compare: (<)Q:\VadoseCase1\Flow\yMesh.dat (1062 bytes)
with: (>)Q:\VadoseBaseCase\Flow\yMesh.dat (1062 bytes)
The files are identical
```

Base Case vs. Case 2

```
Compare: (<)Q:\VadoseCase2\Flow\yMesh.dat (1062 bytes)
with: (>)Q:\VadoseBaseCase\Flow\yMesh.dat (1062 bytes)
29c29
< 0 5 c prev 1.5 2.54 10 !Roof
---
> 0 5 c prev 1.5 2.54 7 !Roof
```

Base Case vs. Case 3

```
Compare: (<)Q:\VadoseCase3\Flow\yMesh.dat (1062 bytes)
with: (>)Q:\VadoseBaseCase\Flow\yMesh.dat (1062 bytes)
21c21
< 0 6 c prev 1.4 2.54 10 !Vessel Floor
---
> 0 6 c prev 1.4 2.54 5 !Vessel Floor
```

Base Case vs. Case 4

```
Compare: (<)Q:\VadoseCase4\Flow\yMesh.dat (1062 bytes)
with: (>)Q:\VadoseBaseCase\Flow\yMesh.dat (1062 bytes)
17c17
< 1 30.48 -22 !Watertable
---
> 1 30.48 -42 !Watertable
```

The differences encountered in Case 2, Case 3, and Case 4 correctly reflect the changes in these cases as specified in Table 1 and *Mesh_Geometry_Rev0.xls*.

mtypMesh.dat: I quite don't understand the zone indices from x and y mesh input. How are they different from the element indices.

Zone indices identify areas of the mesh that have the same material. As seen in the xMesh.dat and yMesh.dat files, each of these material zones is subdivided into element meshes. For example, in xMesh.dat, the first Saltstone region has 60 elements in the radial direction.

mtypMesh.dat were compared for all cases. The results are given below.

Base Case vs. Case 1

```
Compare: (<)Q:\VadoseCase1\Flow\mtypMesh.dat (1173 bytes)
  with: (>)Q:\VadoseBaseCase\Flow\mtypMesh.dat (1175 bytes)
37,41c37,41
< 0  2  2  4  4  6  !inner floor joint
< 0  2  2  10 10 15 !inner roof joint
< 0  4  4  5  9 19 !support column
< 0  6  6  4  4  6  !middle floor joint
< 0  6  6  10 10 15 !middle roof joint
---
> 0  2  2  4  4  18 !inner floor joint
> 0  2  2  10 10 18 !inner roof joint
> 0  4  4  5  9 19 !support column
> 0  6  6  4  4  18 !middle floor joint
>0  6  6  10 10 18 !middle roof joint
```

Base Case vs. Case 2

```
Compare: (<)Q:\VadoseCase2\Flow\mtypMesh.dat (1175 bytes)
  with: (>)Q:\VadoseBaseCase\Flow\mtypMesh.dat (1175 bytes)
The files are identical
```

Base Case vs. Case 3

```
Compare: (<)Q:\VadoseCase3\Flow\mtypMesh.dat (1175 bytes)
  with: (>)Q:\VadoseBaseCase\Flow\mtypMesh.dat (1175 bytes)
The files are identical
```

Base Case vs. Case 4

```
Compare: (<)Q:\VadoseCase4\Flow\mtypMesh.dat (1175 bytes)
  with: (>)Q:\VadoseBaseCase\Flow\mtypMesh.dat (1175 bytes)
The files are identical
```

The differences encountered in Case 1 correctly reflect the changes in this case as specified in Table 1.

3. Examine the Mesh2d plots available in the \Flow subdirectories and verify that the computational mesh is correct.

Extent of model (axial) in *Mesh_Geometry_Rev0.xls* is not reflected in Mesh2d plots.

The radial extent of the model should be 8051.80 cm. Using TechPlot the model extent appears to be 8049.44. Is this what you found? Possibly the model domain is off by 1 cm but I don't think that will affect the results. I will double check the zone boundaries for the next set of calculations.

The Mesh2d plots were visually checked and seem to correctly reflect the geometry and the material types specified.

How did you generate the "COOR.dat" and "TYPE.dat" files?

This is automatically done by the Mesh2d code.

4.0 PORFLOW Flow Calculations

Within the \Flow directory for each case a subdirectory is created that holds the individual PORFLOW flow calculations. These subdirectories are named: BaseCase, Case1, Case2, Case3, and Case4 for the separate cases. For all cases 42 steady-state flow calculations were made covering the time period from time zero to 20,000 years. Within each case subdirectory are 42 subdirectories named TI01 through TI42 that contain the input and output files from the PORFLOW flow calculations. For the five cases, a total of 210 flow calculations were made. The PORFLOW run.dat files were created automatically; therefore, spot checking a random selection of cases should be sufficient to uncover any errors. For each case:

1. Check the run.dat files used for flow calculations for approximately 10% of the runs (i.e. four or five) inputs.

In each case, run.dat files for flow calculations were checked for TI01, TI10, TI20, TI30 and TI40. Hence, a total of 25 runs (i.e., 11.9% of the runs) were checked.

Infiltration rate at the top was set at 0.0029 cm/yr (TI01). I thought rainfall at SRS has been commonly set at 28.6 cm/yr. LUDE matrix solver is slow and memory intensive if the problem exceeds 20,000 elements (your problem has > 50,000 elements). Have you tried BLOC solver?

The solution was indeed slow at later times. I will try the BLOC solver for the next set of calculations.

The SOLVe command is not correct

```
!      auto?  period timeStep      multiplier      maxDt  minDt  divisor maxSteps
SOLVe  MANUal 1.e+8  1.e-4        1            1.e+12 1.e-12 1         100
```

When MANUal modifier is used, only 5 numerical inputs are required (See Porflow command SOLVE, Mode 1)

The SOLVe commands came from Greg Flach and Jeff Jordan and are a scheme they had success with. The flow solution uses the first branch of the IF test (i.e. IF (SOLVSS = YES) THEN) so the SOLVe command you point to is not used.

Case 2 vs. Base Case: Why are hydraulic conductivity values slightly different (i.e., 2.936E-3 in Case 2 vs. 2.937E-3 in Base Case) for ID=ROOF at TI01? I thought the thickness was different, but hydraulic conductivity property is the same.

Case 3 vs. Base Case: Again not just the thickness, but hydraulic conductivity values are also different for ID=FLOOR at TI01 (2.959E-3 in Case 3 vs. 2.937E-3 in Base Case).

For the roof and floor, I used a method from Greg Flach to calculate concrete degradation over time. The conductivity should increase over time. The small differences at TI01 come from reading values from the spreadsheets where these calculations were made. I think the calculation is performed at the mid-point in time so some small increase will occur even at TI01.

2. Check approximately 10% of the run.out files generated by the flow calculations to verify that the calculation converged and that the run completed correctly.

In each case, run.out files for flow calculations were checked for TI01, TI10, TI20, TI30 and TI40. Hence, a total of 25 runs (i.e., 11.9% of the runs) were checked. In all cases, steady-state converged solution was achieved, and the run completed correctly.

3. Use the Techplot plot.lay and fcnet.lay plots to verify that the flow solutions converged

In each case, fcnet.lay plots for TI01, TI10, TI20, TI30 AND TI40 were spot checked. When a steady-state converged solution is achieved, fcnet approaches 0. All fcnet.lay plots correctly display the converged flow solution.

5.0 PORFLOW Transport Calculations

Within the \Transport directory for each case a subdirectory is created that holds the individual PORFLOW transport calculations. These subdirectories are named: BaseCase, Case1, Case2, Case3, and Case4 for the separate cases. Each case subdirectory will have a subdirectory named \SDU6 which will in turn contain subdirectories for each radionuclide run by PORFLOW. For purposes of this design support calculation, the following nine key radionuclides were run: I-129, Tc-99, Np-237, Pu-238, Ra-226, Th-230, U-234, U-235, and Pa-231 giving a total of 45 transport calculations. The PORFLOW run.dat files were created automatically; therefore, spot checking a random selection of cases should be sufficient to uncover any errors. For the transport calculations:

1. Check at least one run.dat file for each case. Also, check at least one run.dat file for each radionuclide. Verify that the input data is correct.

For each case, run.dat files for all radionuclides were checked. As in the flow calculations, LUDE matrix solver was selected. LUDE is slow and memory intensive if the problem exceeds 20,000 elements (your problem has > 50,000 elements). Use of BLOC solver is recommended. In the case of Tc-99, DIST command was used for material types 6-15, and 19. Greg Flach tested this command a few years ago and encountered some problems. I assume DIST work fine now.

Thanks for the observation. Some of the flow and transport runs (see below) did take a very long time to complete. I will try your suggestion for the next set of calculations. I used the DIST command since I found it in an example Saltstone PORFLOW input provided by Greg Flach and Jeff Jordan. While I didn't see any problems, I will check with Greg and Jeff on this point.

2. Check at least one run.out file for each case. Also, check at least one run.out file for each radionuclide. Verify that the runs completed correctly.

For each case, run.out files for all radionuclides were checked. All runs completed normally and correctly, except the Tc-99 runs:

Base case: run.out for Tc-99 stopped at 12,000 years.

Case 1: run.out for Tc-99 stopped at 12,000 years.
Case 2: run.out for Tc-99 stopped at 12,100 years.
Case 3: run.out for Tc-99 stopped at 12,250 years.
Case 4: run.out for Tc-99 stopped at 11,900 years.

Tc-99 was running very slowly so I ended up terminating all of the Tc-99 runs at approximately 12,000 years

Thong Hang's Final Comment

Frank,

I find your responses adequate. The issues were addressed to my satisfaction.

DISTRIBUTION:

SRNS

R. S. Aylward, 773-42A
H. H. Burns, 773-41A
A. D. Cozzi, 999-W
D. A. Crowley, 774-43A
G. P. Flach, 773-42A
K. M. Fox, 999-W
S. J. Hensel, 703-41A
J. M. Jordan, 703-41A
S. L. Marra, 773-A
M. G. Serrato, 773-42A
F. G. Smith, 703-41A
C. Wilson (1 file copy & 1 electronic copy), 773-43A – Rm. 213

SRR

T. C. Baughman, 707-14E
S. D. Burke, 766-H
G. B. Clendenen, 707-14E
T. W. Coffield, 705-1C
R. D. Freeman, 705-1C
K. A. Hauer, 705-1C
T. H. Huff, 707-14E
K. M. Lancaster, 766-H
K. H. Rosenberger, 705-1C
R. E. Sheppard, 705-1C
F. M. Smith, 705-1C